INTERNATIONAL JOURNAL OF SCIENCE AND NATURE

www.scienceandnature.org

DIRECT DETECTION OF PHOTONS FROM EXOPLANETS OF A HOST STAR LEADING TO STUDY ITS ELEMENT COMPOSITIONS

A. T. Mohammed
Department of Astronomy, College of Science,
University of Baghdad, Iraq.

ABSTRACT

Computer simulations of direct detection of photons from an exoplanet that hidden in the diffraction side loops of the host star are presented. This involves computing the point spread function and the modulation transfer function of a Dirac delta function that observed by optical telescope. Jacquinot Gaussian apodization aperture is suggested to bring the exoplanet up the diffraction loops of the parent star and becomes ready for spectroscopic observations owing to study its element compositions. This approach is capable of detecting exoplanets with angular separation of 4λ/D at contrast ratio of 10 ·and it is very easy to be manufactured.

KEY WORDS: Mathematical Modeling, Coronagraphy, Optical Imaging, Fourier Optics, Exoplanets Detection.

INTRODUCTION

The purpose of direct imaging of an exoplanets is to measure its photon flux leading to understand its physical and chemical properties. For example, we can characterize the planet in terms of mass, radius, effective temperature, age, element or molecular compositions. For earth like planets, we can also search for habitability in terms of a surface temperature and pressure that permits liquid water as sign of life. A direct image of exoplanet permits us to obtain a spectrum, using a conventional spectrometer or an integral field spectrometer. To know more about the molecular or element structure of the universe, it is important to study the spectroscopic observations of these planets (Traub, 2010). Therefore, it is so important to reveal those planets and make them possible for spectroscopic observations which is really very difficult task and needs very sophisticated modeling and simulations to overcome this kind of problem. A large number of extrasolar planets have been discovered in the last fifteen years through indirect methods. We have been confirmed the existence of more than 3000 exoplanets, in orbit around just over 1100 stars (Rice, 2014). Direct imaging involves observing the brightness distributions of an extrasolar planet that is located very close to its parent star. Apodized square aperture was suggested to detect a planet with angular separation (***d***) of 4λ/D and at a contrast ratio (***C***) of 10^{-10} (Nisenson, 2001). It has been shown that an achromatic apodized pupil is suitable for imaging extrasolar planets could be obtained by reflection of an unapodized flat wave front on two mirrors (Guyon, 2003). A new class pupil masks have been used to produce point spread function, *psf*, having annular dark zones (Vanderbei 2003).

Several different apodization approaches have been examined to achieve high contrast imaging based on the char acterization of the pupil transmission function rather than masking the star in the image plane (Kasdin, 2003). Another suggested approach is to optimize the two-dimensional pupil apodizations using arbitrary apertures to achieve high contrast detection. This approach produces a 2-D shaped pupil with no simplifying geometric assumptions (Carlotti, 2011). Super Gaussian apodization functions in the telescope pupil plane or in the coronagraph Lyot plane has been introduced to improve the imaging contrast (Cagigas, 2013). An apodized pupil Lyot coronagraph in the context of exoplanet imaging with ground based optical telescopes has been examined. This combines an apodization in the pupil plane with a small Lyot mask in the focal plane of the instrument (Martinez, 2007). A hybrid coronagraph configuration that uses a shaped pupil as the apodizing mask in a Lyot-style architecture is managed to surpasses 10^{-9} contrast starting from an angular separation of 2λ/D (Zimmerman, 2016). Another solution was proposed for apodized pupil Lyot coronagraph with segmented aperture telescopes to remove broadband diffraction light from a star with a contrast level of 10^{-10} (Mamadou, 2016). Despite these discoveries, imaging of extrasolar planets is still very challenging task because of the planet-star luminosity contrast ratio (10^{-6} for young giant planets and down to 10^{-8}-10^{-10} for old giant and rocky planets). Generally one needs a technique that is effective enough to capture the weak light photons of a very faint planet.

The search for Earth-like planet requires a contrast level of ~ 10^{-10} and a separation of a few λ/D from the center of the star. Imaging with optical telescope is not offering such observations. This is due to the fact that the aperture of the telescope creates a side loops attenuation pattern called Airy disc in which the brightness distributions of the planets are totally attenuated. The aim of this work is to set a mathematical model for observing extrasolar planet by optical telescope. This involves computing the *psf* of a Dirac delta function and also computing the corresponding modulation transfer function (*MTF*). The visualize model also involves suggesting a simple approach that apodize Jacquinot aperture with a normal Gaussian function. The standard deviation of this function (σ) is then optimized with respect to achieve as minimum inner working distance as possible.

Numerical simulations and results:

First of all, lets us start with identifying the problem of imaging extrasolar planet in the vicinity of a hosted star. We assume the *psf* of an optical system is a two-dimensional *sinc* function given by:

$$psf\,(x,y)=\left|\,\sin(\text{®}\,r)/(\text{®}\,r)\right| \qquad \text{for } r \text{ not equal zero} \tag{1}$$
$$psf\,(x,y)=1 \qquad \text{for } r=0$$

where

$$r=\left[(x-x_c)^2+(y-y_c)^2\right]^{1/2}$$

x and *y* are taken to be a mesh grid of length -20 : 20 and x_c , y_c are the coordinates of the central point of an array. The result of computing Eq.(1) is shown in Fig.(1) and the central plot through Fig.1 is shown in Fig.2.

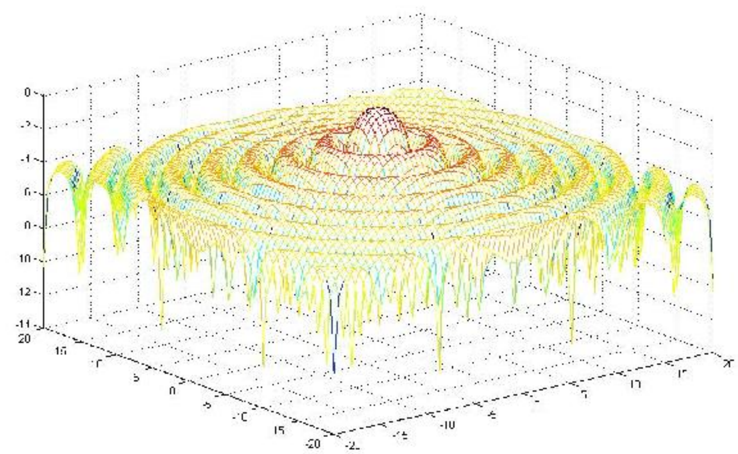

FIGURE 1: *psf* computing from Eq.(1).

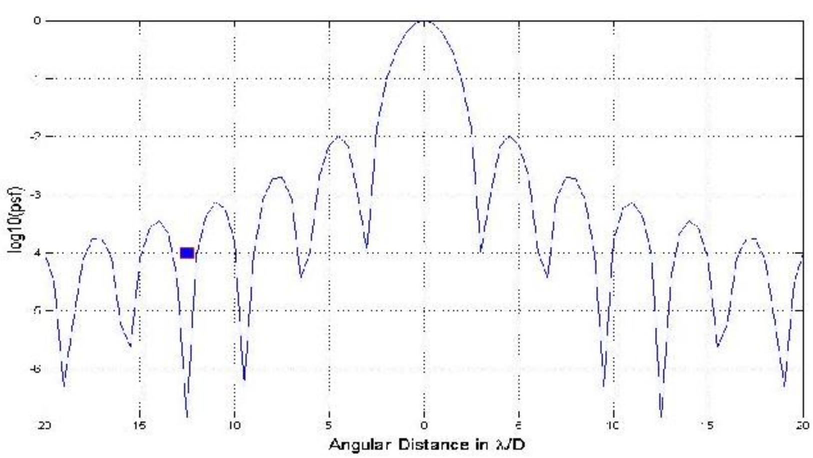

FIGURE 2: Central line through Fig.1.

It is so clear that observing exoplanets with ***d***=4λ/D and C below 10^{-4} is impossible. We are looking for an optical telescope that is being capable of revealing exoplanets from the diffraction side loops of a hosted star.

Computer simulations are carried out to investigate the possibility of imaging exoplanets by optical telescope. Let us start with a simple imaging model by assuming the pupil function of an optical telescope is a circular function of constant values, i.e.

$$A(\text{¸},\text{¥})=\begin{cases}1 \text{ if } r\le \mathrm{R}\\ 0 \text{ otherwise}\end{cases} \tag{2}$$

where R is the radius of the optical telescope. The *psf* of any optical imaging system that observing a Dirac delta function by optical telescope is the absolute of the square Fourier transform of the pupil function.

$$psf(x,y)=\left|FT(A(¸,¥)\right|^{2} \qquad (3)$$

The corresponding optical transfer function is the autocorrelation of the pupil function (Mohammed 1990),

$$T_{\circ}(u,v)=\int_{-\infty}^{\infty}\int_{-\infty}^{\infty}A(¸,¥)A*(¸-\bar{¸},¥-\bar{¥})d\bar{¸}d\bar{¥} \qquad (4)$$

Where FT denotes Fourier transform operator and *MTF* is the absolute of $T_{\circ}(u,v)$. The pupil function, $A(¸,¥)$, is taken to be a circular function of diameter R and of unity magnitude inserted in an array of size N by N pixels padded with zeros. The *psf* is then computed via Eq.(3) using diameters D=60, 120, 180, 240 pixels. The surface plot of the central region of the *psf* for different D is shown in Fig (3). The surface plots of the central regions of log10 (*psf*) are shown in Fig. (4).

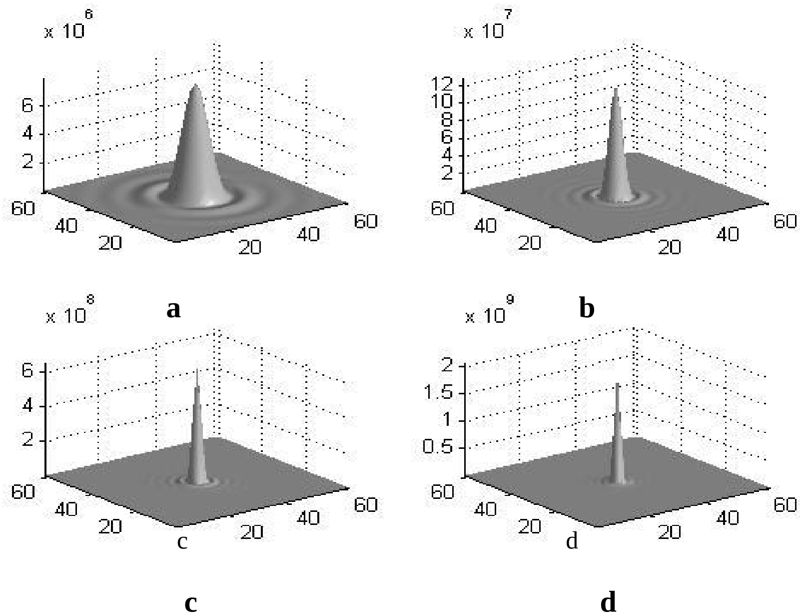

FIGURE 3. Surface plots of the central region of the *psf* for different D, a- D=60, b- D=120, c- D=180, d- D=240.

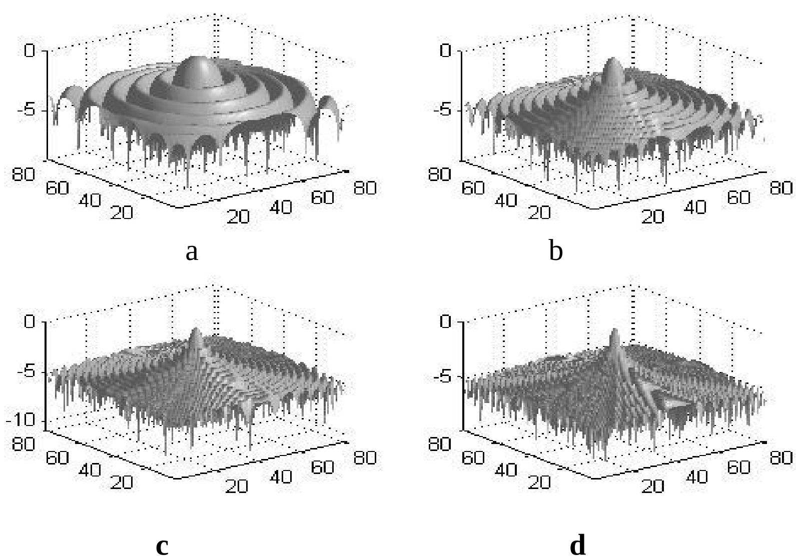

FIGURE 4. Surface plots of the central regions of log10(*psf*) for different D, a- D=60, b- D=120, c- D=180, d- D=240.

The central line through log10(*psf*) for different D are shown in Fig. 5.

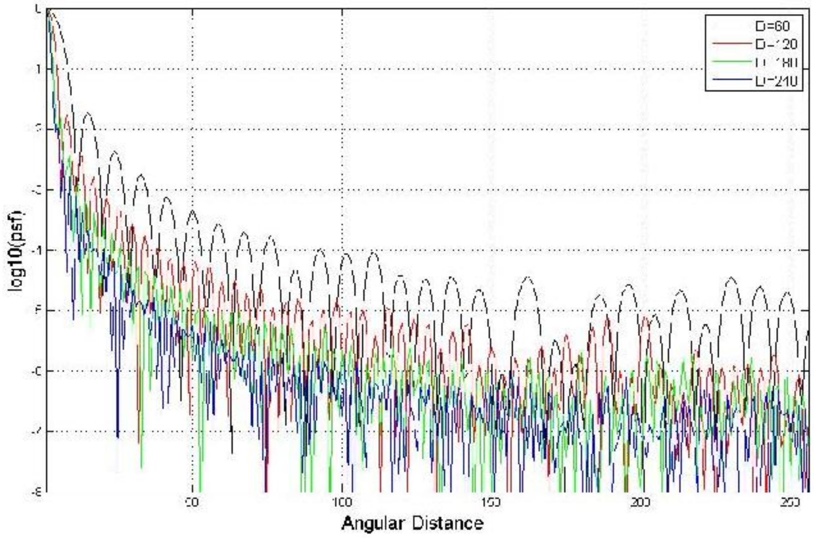

FIGURE 5: Central lines through log10(*psf*) for different D.

The *MTF* of a Dirac delta function that observed by optical telescope are shown in Fig.6 and their central lines are shown in Fig.7

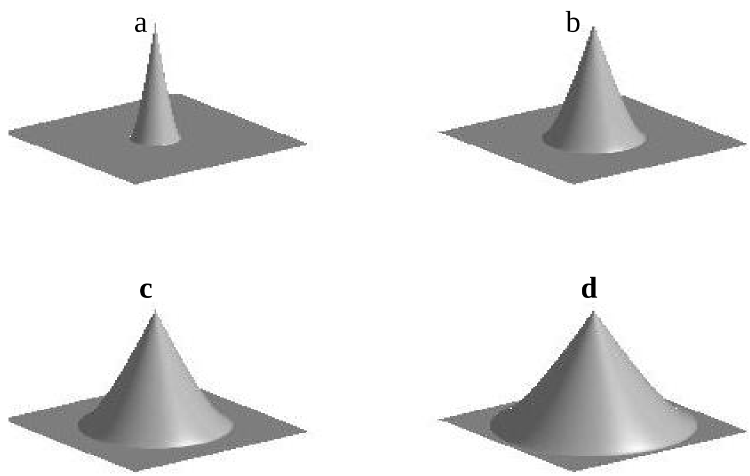

FIGURE 6. *MTF* for different D, a- D=60, b- D=120, c- D=180, d- D=240.

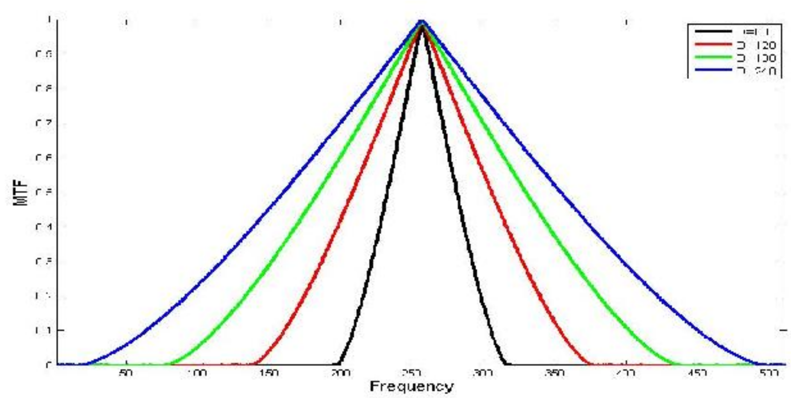

FIGURE 7. Central plots through Fig.6.

It is so clear that even with using large optical telescope, the side loops of the *psf* of the star is not decline significantly. The *MTF* shows significant gain of information with large telescope.

To assess the quality of these apertures on observing exoplanets, the star and the planet are assumed to be a binary system of two Dirac delta functions separated by an angular separation ***d***. The brightness of the star is one and the brightness of the planet has a certain value of ***C*** (***C***<<1).

$$\text{Image}\,(x, y)=psfn(x, y)+C*psfn(x-\boldsymbol{d}, y-\boldsymbol{d}) \qquad (5)$$

Where *psfn* is the *psf* that normalized to one at its maximum value. The image is also normalized to one at its maximum value and log10 is then taken. The result demonstrates the central region of the image of a binary system that observed by optical telescope of different diameters.

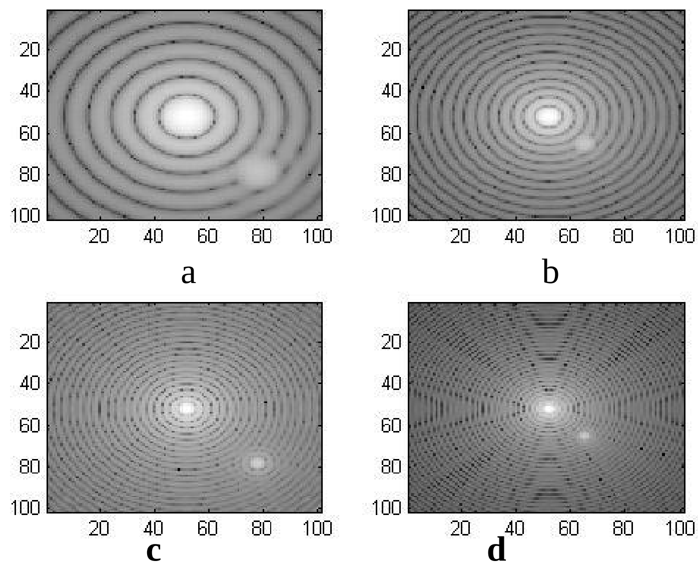

FIGURE 8. Planet detection with ***d***=4λ/D and ***C***=10^{-2} for different D, a- D=60, b- D=120, c- D=180 d- D =240.

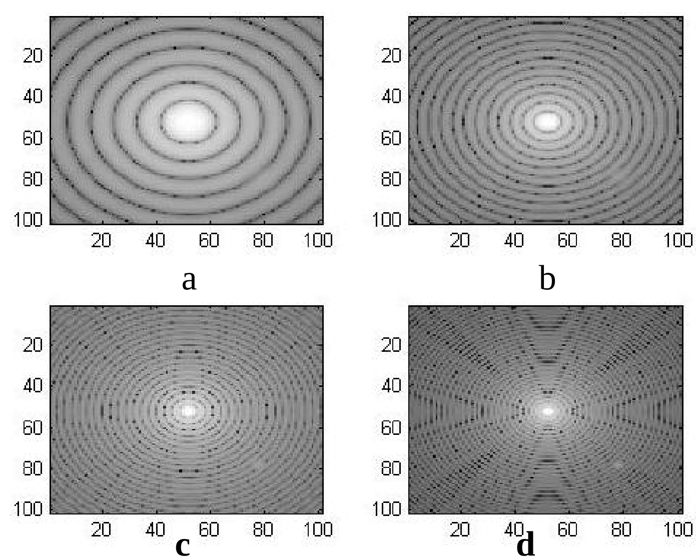

FIGURE 9. Planet detection with ***d***=4λ/D and ***C***=10^{-5} for different D, a- D=60, b- D=120, c- D=180, d- D=240.

These two figures demonstrate very clearly that as the telescope diameter increases, the planet becomes sharper and the inner working distance (the distance from the center of star to 1λ/D) gets smaller. Optical telescopes with diameters D==240 are capable of detecting planet with ***C***=10^{-5}. We are looking for the requirements of an optical telescope that is being able to provide a high contrast observation. Jacquinot pupil function (Cagigas 2003) has proven to offer a sharp inner working distance than others. This is why we are choosing this pupil function.

$$|\gamma| < R\ [\ \exp\left(-\left(\frac{\alpha\zeta}{R}\right)^2\right) - \exp(-\alpha^2)\ ] \qquad (6)$$

This means that if Eq.(6) is satisfied, then the pupil function is equal to one otherwise is equal to zero. The pupil function and its log10 (*psf*) are shown in Fig.10.

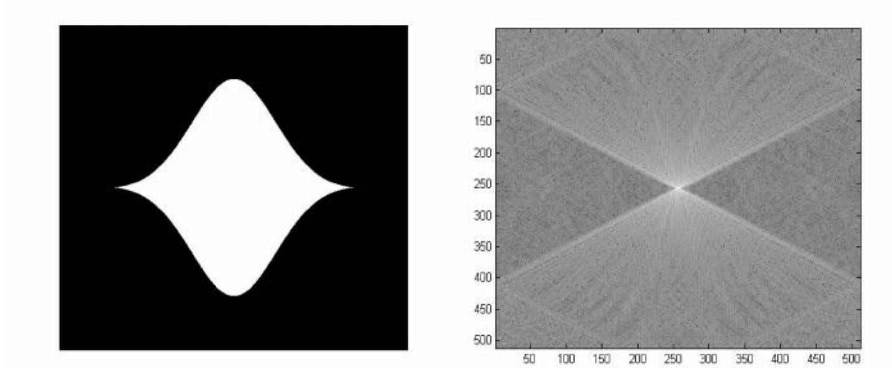

FIGURE 10. Jacquinot pupil function (left) and its log10(*psf*) (right)

The new suggested approach involves setting a Gaussian of the form $G(x,y)=exp(-r^2/2\sigma^2)$ inside the Jacquinot pupil function. It should be pointed out here that the optimum value of σ is taken according to achieve as a minimum inner working distance as possible. The optimum value was found to be 33 pixels. The horizontal and vertical plots of the log10 (*psf*) of the normal Jacquinot aperture and the Gaussian apodization aperture are shown in Fig.11. The image of star and planet for different values of ***C*** are shown in Fig.12.

.

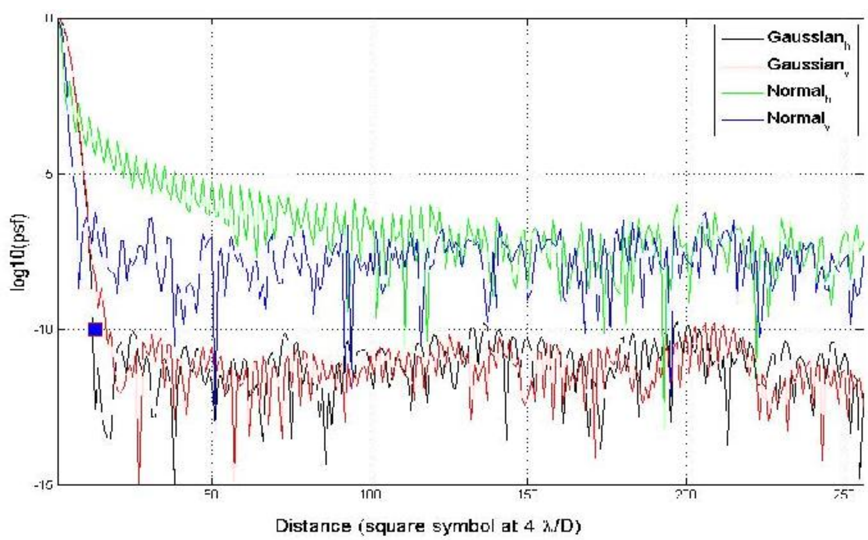

FIGURE 11. Log10**(***psf***)** with normal and apodized Jacquinot apertures. The square is just an indication of the location of the plan for $\boldsymbol{d=4\lambda/D}$ and $\boldsymbol{C}=10^{-10}$.

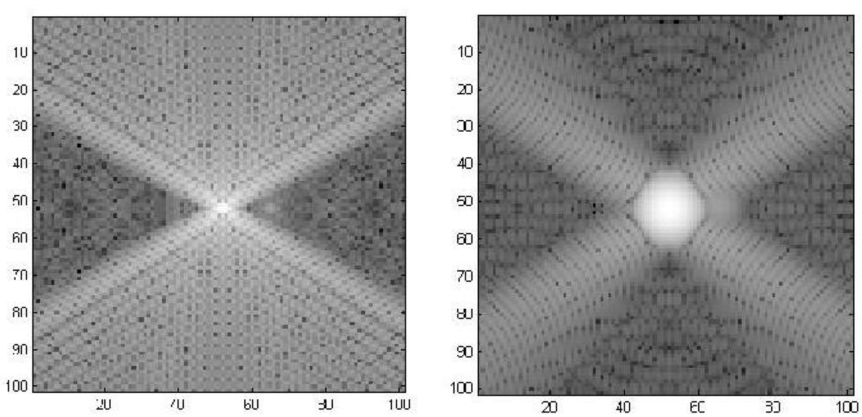

FIGURE 12. Recovering the planet with normal Jacquinot pupil with $\boldsymbol{d=4\lambda/D}$, $\boldsymbol{C}=10^{-5}$ (left) and the new adopted method with $\boldsymbol{d=4\lambda/D}$, $\boldsymbol{C}=10^{-9}$ (right) .

It is so clear that the normal Jacquinot pupil is hardly recover the planet with $\boldsymbol{C}=10^{-5}$ while the adopted method clearly recover the planet with $\boldsymbol{C}=10^{-7}$. The diagonal lines of the star and planet with different values of ***C*** are shown in Fig.12.

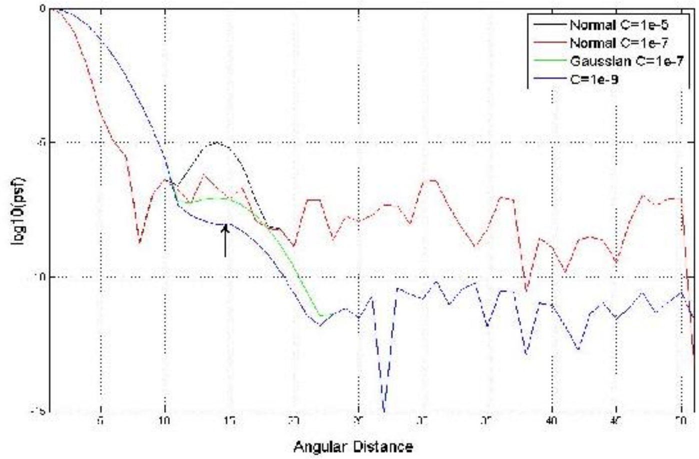

FIGURE 13. Central lines through star and planet for different values of ***C***. The arrow indicates the location of the planet.

The results demonstrate the capability of this new adopted method for resolving exoplanets even with $\boldsymbol{C}=10^{-10}$.

CONCLUSION

The results indicate that exoplanets with $\boldsymbol{d}=4\lambda/D$ and $\boldsymbol{C} < 10^{-5}$, optical telescope is not capable of resolving exoplanets even if we increase the size of the telescope five times. Jacquinot pupil is manage to detect exoplanets with $\boldsymbol{C}=10^{-5}$ and hardly detecting planet with $c=10^{-6}$ while the new adapted method being able to detect planet with $\boldsymbol{C}=10^{-10}$. In real applications when there is a wavefront errors that introduced by atmospheric turbulence, the capability of these method reduced significantly and extreme adaptive optics is not capable of recovering planet beyond $\boldsymbol{C}=10^{-6}$.

This is attributed to the limitations imposed by the *psf* of the optical telescope.

ACKNOWLEDGMENT

I would like to thank Prof. Antonio D'onofrio, the director of the mathematics and Physics department of the seconda universita degli study di Napoli and Prof. Filippo Terrasi for their kind and sincere assistance throughout my sabbatical stay.

REFERENCES

Cagigas M.A., Valle P.J. and Cagigal, M.P. (2013) Super-Gaussian apodization in ground based telescopes for high contrast chronograph imaging. *Optics Express* 10: 12744-12756.

Carlotti, A, Vanderbei, R., and Kasdin, N. J. (2011) Optimal pupil apodization for arbitrary apertures for high - contrast imaging. *Optics Express* 19:26796-26809.

Guyon, O. (2003) Phase Induced amplitude apodization of telescope pupils for extrasolar terrestrial planet imaging. *Astronomy & Astrophysics Journal* 404: 379-387.

Kasdin, N., Vanderbei, R., Spergel D. and Littman, M. (2003) Extrasolar planet finding via optimal apodized-pupil and shaped-pupil chronographs. *The Astrophysical Journal* 582:1147-1161.

Mamadou, N., Soummer R., Laurent P. (2016) Apodized pupil Lyot coronagraphs for arbitrary apertures. V. hybrid shaped pupil designs for imaging Earth-like planets with future space observatories. *Astrophysical J*., 818:163-172.

Martinez, P. (2007) Optimization of apodized pupil Lyot chronograph for ELTs. *Astronomy and Astrophysics Journal* 474:671-678.

Mohammed, A.T., Rashid, N.M. and Sadik, A.R. (1990) Computers Simulations of astronomical objects as seen by ground-based Optical telescopes. *Optics and Laser in Engineering* 12:233-243.

]Nisenson, P. and Papaliolios, C. (2001) Detection of Earth-like planets using apodized telescopes. *The Astrophysical J* 548:L201-L205.

Rice K. (2014) The Detection and Characterization of Extrasolar planets. *Challenges* 5:296-223.

Traub, W.A. and Oppenheimer, B.R. (2010) Direct Imaging of Exoplanets. From Exoplanets, S. Seager, ed. (Tucson: Univ. Arizona Press; 2010).

Vanderbei, R.., Spergel, D. and Kasdin, N. (2003) Circularly symmetric apodization via starshaped mask. *Astrophysical Journal* 59:686-694.

Zimmerman N. (2016) Shaped pupil Lyot coronographs: high contrast solutions for restricted focal planes. *J. Astron. Telesc. Instrum. Syst*. 2(1): 011012.